

# Processing and ferroelectric behavior of textured $\text{KSr}_2\text{Nb}_5\text{O}_{15}$ ceramics

Cihangir Duran

Received: 9 September 2005 / Accepted: 23 November 2005 / Published online: 26 September 2006  
© Springer Science+Business Media, LLC 2006

**Abstract**  $\langle 001 \rangle$ -textured  $\text{KSr}_2\text{Nb}_5\text{O}_{15}$  (KSN) ceramics were fabricated in a matrix of  $\text{SrNb}_2\text{O}_6$  and  $\text{KNbO}_3$  powders via reactive templated grain growth (TGG), using  $\langle 001 \rangle$ -oriented acicular KSN particles as the template for grain growth. KSN phase formation started at 1100 °C and was complete at 1300 °C. Template particles grew at the expense of matrix grains with increasing sintering time and temperature, resulting in improved texture fraction,  $f$ . A maximum fraction of 0.98 was obtained in 1.5 wt%  $\text{Nb}_2\text{O}_5$  and 10 wt% template containing samples sintered at 1450 °C for 6 h. A template content of 10 wt% resulted in a high quality of texture with a narrow distribution of elongated grains in [001]. The highly textured ceramics ( $f \geq 0.9$ ) had a remanent polarization of 0.19 C/m<sup>2</sup> in the polar  $c$  direction, [001], as compared to 0.03 C/m<sup>2</sup> in the non-polar  $a$  or  $b$  direction and 0.04 C/m<sup>2</sup> as for the random sample. The estimated saturation polarization ( $P_{\text{sat}}$ ) was 0.25 C/m<sup>2</sup> which is comparable to reported KSN single crystal value of 0.25 C/m<sup>2</sup>. This indicates that TGG is a viable method to fabricate textured ceramics having ferroelectric properties close to the single crystals.

## Introduction

$(\text{K,Sr})\text{Nb}_5\text{O}_{15}$  is a solid solution having tetragonal tungsten bronze (TTB) crystal structure when  $\text{SrNb}_2\text{O}_6$  content is between nearly 59–78 mol% [1].  $\text{KSr}_2\text{Nb}_5\text{O}_{15}$  (stoichiometric composition with 66.7 mol%  $\text{SrNb}_2\text{O}_6$ , abbreviated as KSN) single crystal is a uniaxial ferroelectric with 4 mm symmetry and therefore shows enhanced ferroelectric and piezoelectric properties only in [001] (e.g., two allowed polarization directions) [2]. KSN exhibits a room-temperature electrooptic effect nearly an order of magnitude greater than that of  $\text{LiNbO}_3$  [1]. In addition, alkali and alkaline earth cations can be accommodated (or doped) in the TTB structure and therefore a wide spectrum of Curie temperatures ( $T_c$ ) and electrical properties can be realized [2, 3].

Randomly oriented polycrystalline KSN ceramics show inferior electrical properties compared to the KSN single crystals due to abnormal grain growth that inhibits densification [4] and limited numbers of polarization directions [2]. In addition, each grain in the polycrystalline sample has a crystallographic orientation different from the neighboring grains, resulting in an averaging of electrical properties in all directions. Texturing of the material in the [001] would impart a macroscopic symmetry ( $\infty m$  for textured and poled ferroelectric ceramics) that is anisotropic in nature. Depending upon the poling and measurement directions, the properties would reflect this macroscopic symmetry. In this case, measuring along the [001] would show enhanced polarization and dielectric constant. Templated grain growth (TGG) method has been successfully applied to fabricate textured ceramics [5–11]. TGG is an inexpensive method to produce a texture in the desired crystallographic direction in a

---

C. Duran (✉)  
Electronic Materials Laboratory,  
Department of Materials Science and Engineering,  
Gebze Institute of Technology,  
P.K. 141, 41400, Gebze-Kocaeli, Turkey  
e-mail: cduran@gyte.edu.tr

polycrystalline body. Anisotropically shaped template particles (i.e. whisker or platelet) are aligned in a fine-grained matrix by shear-forming methods such as tape casting and then they preferentially grow at the expense of matrix grains during sintering. The final texture in the ceramic depends strongly on the initial concentration of template particles [7, 11].

There are limited numbers of results on textured KSN ceramics. Kimura et al. [12] obtained 86% texture, as measured by the Lotgering factor, by two-stage hot pressing, without using any templates. They reported anisotropic dielectric properties as a result of texture in the microstructure. Yurdal et al. [13] reported fabrication of highly textured KSN ceramics, using acicular KSN templates. Other textured systems with a TTB crystal structure include hot-pressed  $\text{Sr}_x\text{Ba}_{1-x}\text{Nb}_2\text{O}_6$  ( $x = 0.30\text{--}0.65$ ) (SBN30-SBN65) [14], hot-pressed  $\text{Pb}_{0.60}\text{Ba}_{0.40}\text{Nb}_2\text{O}_6$  [15] and TGG of SBN40 [16].

Reactive sintering was found to be advantageous as compared to conventional sintering in that the latter resulted in low densification and cracking due to abnormal grain growth [17–19]. Chemical reaction and densification are both achieved in the same heat treatment in reactive sintering. These two steps can occur in sequence or concurrently, depending on the material and processing variables [20]. Typically, reactive sintering is done by sintering either the constituent oxides or intermediate products, which eliminates the prereaction (or calcination) step(s) and induces an additional driving force for sintering due to the free energy of the chemical reaction [17]. Reactive sintering has been successfully applied to ceramics having TTB structure [13, 17–19].

In a recent paper, texture development in [001] as a function of sintering conditions and presence of excess  $\text{Nb}_2\text{O}_5$  in the reactive matrix were reported, using only 10 wt% template particles [13]. In this study, phase formation from a reactive matrix of  $\text{KNbO}_3$  and  $\text{SrNb}_2\text{O}_6$ , and texture development as a function of template contents (0, 5, 10, 15 wt%) are investigated to fabricate <001>-textured KSN by reactive TGG. Excess  $\text{Nb}_2\text{O}_5$  (0, 1, 1.5 wt%) is added to form a liquid during sintering. The effect of  $\text{Nb}_2\text{O}_5$  doping on phase formation and microstructure development as well as anisotropic electrical properties (e.g., polarization vs. electric field) induced by texturing are also reported here.

## Experimental procedures

$\text{KSr}_2\text{Nb}_5\text{O}_{15}$  (KSN) ceramics were prepared by reactive sintering of  $\text{SrNb}_2\text{O}_6$  (SN) and  $\text{KNbO}_3$  (KN)

powders. SN or KN was first synthesized by solid-state reaction of  $\text{SrCO}_3$  (Alfa) or  $\text{K}_2\text{CO}_3$  (Merck) and  $\text{Nb}_2\text{O}_5$  (Aldrich) at 1050 °C for 5 h and 900 °C for 1 h, respectively. Appropriate amounts of SN and KN powders together with excess  $\text{Nb}_2\text{O}_5$  (0, 1, 1.5 wt%) were first dispersed in distilled water with ammonium salt of poly(acrylic acid) (PAA-NH<sub>4</sub>; Darvan 821A, R.T. Vanderbilt) by ball milling for 24 h, and then mixed with polyvinyl alcohol (PVA) (Sigma), glycerol (Aldrich) and KSN templates (0–15 wt%). Template particles were incorporated into the slurry at this stage so as not to cause template breakage during ball milling. The slurry was further stirred for 24 h in a closed beaker for homogenous mixing of polymers and ceramics. Several drops of ethylene glycol surfactant (Surfynol 104E, Air Products) were added to remove air bubbles formed during mixing. Tape casting slurries showed a pseudoplastic behavior. A detailed study of tape casting process was given elsewhere [13]. After binder burnout, samples were heated at 7 °C/min to 1350–1450 °C and held for 2–6 h. The density of the samples was determined using the Archimedes' technique.

The acicular KSN particles were used as templates for the reactive TGG experiments. They were synthesized by reacting KCl salt with SN mixed at a weight ratio of 1.25–1. This mixture was heated to 1100 °C in a closed  $\text{Al}_2\text{O}_3$  crucible, kept for 6 h and finally cooled to room temperature at a rate of 2 °C/min. As-synthesized particles were washed several times with hot distilled water to remove the remaining salt on the particles. Templates of 1–3 μm in diameter and 10–30 μm in length, as confirmed by Scanning Electron Microscopy (SEM) (Philips XL30), were physically separated by differential settling in water to narrow the texture distribution in the final sintered KSN ceramics. X-ray diffractometry (XRD) (Rigaku) showed that template particles consist of minor amounts of  $\text{Sr}_2\text{Nb}_2\text{O}_7$  (JCPDS No. 28-1246) together with the KSN phase (JCPDS No. 34-108). The fiber axis is along the [001] (or *c* direction) crystallographic direction.

Table 1 summarizes the sample designation, excess  $\text{Nb}_2\text{O}_5$  content and initial amounts of templates in the KSN samples. In nomenclature, N refers to excess  $\text{Nb}_2\text{O}_5$  and T refers to template content. For example, excess  $\text{Nb}_2\text{O}_5$  is 1 wt% and template content is 10 wt% in the N1-T10 samples.

Amount of KSN phase formation from a reactive mixture of SN and KN was calculated as a function of excess  $\text{Nb}_2\text{O}_5$  content in the random samples. The samples were heated at 7 °C/min to temperatures between 1000 °C and 1400 °C, and then air-quenched. The quenched samples were ground for XRD analysis.

**Table 1** Sample designation, template content, and excess Nb<sub>2</sub>O<sub>5</sub> amount in KSN ceramics

Sample designation	Excess Nb <sub>2</sub> O <sub>5</sub> , wt%	Template content, wt%
N0-T0	0	0
N1-T0	1	0
N1.5-T0	1.5	0
N0-T5	0	5
N0-T10	0	10
N0-T15	0	15
N1-T10	1	10
N1.5-T10	1.5	10

The scan rate was 1°2θ per min with a step size of 0.02°. The strongest line intensities of KSN (2θ = 32.077°) (JCPDS # 34-108), SN (2θ = 29.211°) (JCPDS # 28-1243), and KN (2θ = 31.566°) (JCPDS # 32-0822) peaks were integrated to find the peak areas, using curve fitting. The fraction of KSN formed was calculated by comparing the integrated peak areas of KSN and (SN + KN).

For microstructure analysis, samples were polished to 3 μm using diamond paste and then thermally etched at 50 °C below the sintering temperature for 30 min. Morphological texture was characterized using SEM on samples cut parallel (//) to the casting direction. Crystallographic texture was characterized using XRD on samples cut perpendicular (⊥) to the casting direction and then texture fraction, *f*, was calculated, using the Lotgering factor [21];

$$f = (P - P^\circ)/(1 - P^\circ) \quad (1)$$

where *P* and *P*<sup>°</sup> are  $[I_{(001)} + I_{(002)}]/\Sigma I_{(hkl)}$  in the textured and random cases, respectively. Crystallographic orientation distribution was obtained from corrected rocking-curve measurements [22, 23], using the KSN (002) peak. The orientation distribution was calculated by fitting corrected rocking curves to the March–Dollase equation [24, 25];

$$Q(f, r, \alpha) = f(r^2 \cos^2 \alpha + r^{-1} \sin^2 \alpha)^{-3/2} + (1 - f) \quad (2)$$

where *f* is the texture fraction, *r* is the degree of orientation parameter, and α is the misalignment angle from the texture direction (e.g., [001]). The *r* is closely related to the width of the orientation distribution of the anisotropic grains and ranges from *r* = 1 for random to *r* = 0 for perfectly textured materials.

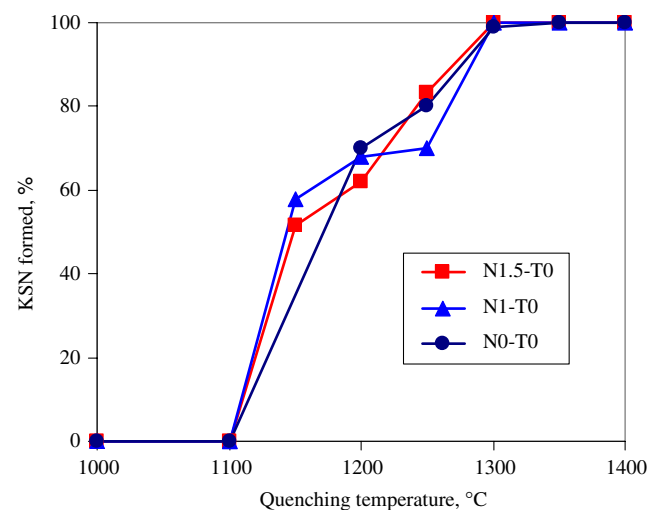
For polarization–electric field (P–E) measurements, samples were electroded with silver and baked at 600 °C for 30 min. The P–E hysteresis loops were measured at 20 Hz at room temperature. Remanent polarization and coercive field were determined from

the P–E loops and compared for random and textured samples.

## Results and discussion

### Phase formation and microstructure evolution in random samples

During reactive sintering, SN and KN react to form final KSN phase with increasing temperature. KSN phase formation was determined from the quenching experiments as a function of temperature and excess Nb<sub>2</sub>O<sub>5</sub> content. Template-free N0-T0, N1-T0, and N1.5-T0 samples were used and heated to desired temperatures (1000–1400 °C) and then air-quenched. KSN phase formation was found to commence at 1100 °C and complete at 1300 °C, regardless of the presence of excess Nb<sub>2</sub>O<sub>5</sub> (Fig. 1). This result indicates that Nb<sub>2</sub>O<sub>5</sub> does not alter the phase formation characteristics (at the resolution limits of the XRD). However, excess Nb<sub>2</sub>O<sub>5</sub> affects the microstructure evolution, as seen from Fig. 2. Anisotropic grain growth becomes more dominant with increasing Nb<sub>2</sub>O<sub>5</sub> content. The grains of a ceramic having the TTB structure grow anisotropically because the growth rate in the *c* direction ([001]) is faster than that in the *a* direction, resulting in acicular (or anisotropic) growth of the grains [12, 26]. This acicular growth is promoted in the presence of a liquid and randomly oriented at the absence of template particles. Note that Nb<sub>2</sub>O<sub>5</sub>-free sample (Fig. 2a) does not undergo severe anisotropic grain growth even though it was sintered at higher temperature (e.g., 1400 °C for 6 h vs. 1350 °C

**Fig. 1** KSN phase formation as a function of quenching temperature and excess Nb<sub>2</sub>O<sub>5</sub> content in the random samples

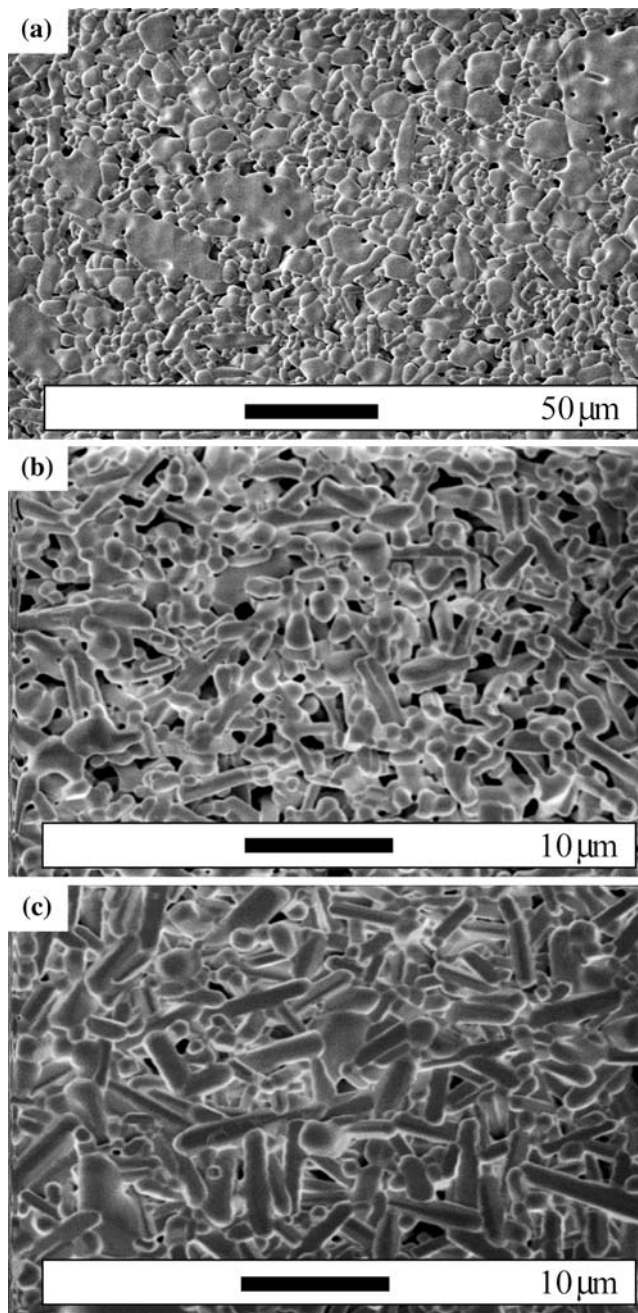


**Fig. 2** Microstructures of random samples as a function of excess  $\text{Nb}_2\text{O}_5$ ; (a) N0-T0 sintered at 1400 °C for 6 h, (b) N1-T0 sintered at 1350 °C for 2 h, and (c) N1.5-T0 sintered at 1350 °C for 2 h

for 2 h). However, a few grains grown abnormally and anisotropically are present, which can be attributed to the formation of a liquid possibly due to local inhomogeneity in chemical composition [1, 4].

#### Texture development and characterization

Figure 3 shows texture evolution in the N0-T10 samples as a function of sintering temperature and time.

Powder pattern (Fig. 3a) is given and main KSN peaks are marked to visualize the texture evolution from the XRD patterns. Figure 3b shows that initially aligned template particles and matrix grains are easily observable after sintering at 1350 °C for 2 h. With increasing sintering temperature and time, template particles grow at the expense of matrix grains and highly textured ceramic is obtained, as reflected by strong (00l) peaks in the XRD patterns and elongated grains in the SEM pictures. Also, the density increased from 64% of theoretical density (TD) at 1350 °C to 88% TD at 1400 °C.

XRD patterns in Fig. 4 compare the texture development as a function of template content. The peaks other than {00l} are dominant in the N0-T5 and N0-T15 samples (Fig. 4a, c), stating that these samples are not as strongly textured as the N0-T10 sample (Fig. 4b) where {00l} are dominant. In other words, a template content of 5 wt% is not enough to induce high texture fraction due to the grain growth in the matrix. Many short and off-axis acicular grains together with some equiaxed grains are present in Fig. 4a. Matrix grain growth competes with the anisotropically growing grains by decreasing the total grain boundary area, thereby decreasing the driving force for TGG. Increasing the template concentration to 10 wt% resulted in better texture development because the larger number of template particles grow at the expense of the fine-grained matrix at shorter time (because of the smaller intertemplate spacing). Increasing the amount of template particles further (to 15 wt%), however, caused tangling of the templates during tape casting. N0-T5 and N0-T10 samples reached a density of ~93% TD and N0-T15 reached a density of 89% TD.

Figure 5 compares the microstructures of random (N1.5-T0) and textured (N1.5-T10) samples sintered at 1400 °C and 1450 °C for 2 h, respectively. A duplex microstructure consisting of bigger (in excess of 100 μm for some grains) and smaller grains develops in the N1.5-T0 (Fig. 5a). Cracking occurs due to high internal stress caused excessively by abnormal grain growth in the microstructure [4, 17]. However, the textured sample exhibits a very uniform microstructure (Fig. 5b), despite the fact that it was sintered at higher temperature. A comparison of random and textured samples indicates that template particles promote the growth and alignment of matrix grains in the direction of the template particles' orientation during heat treatment, thereby regulating the microstructure. Therefore, neither abnormal grain growth nor cracking is observed in the textured samples, prepared by reactive sintering and TGG.

**Fig. 3** Crystallographic (XRD patterns,  $\perp$ -cuts) and morphological (SEM pictures,  $\parallel$ -cuts) texture evolution in the N0-T10 samples sintered at (b) 1350 °C for 2 h, (c) 1350 °C for 6 h, and (d) 1400 °C for 6 h. Curve (a) is given as a reference powder pattern. Main KSN peaks (JCPDS # 34-108) are also marked

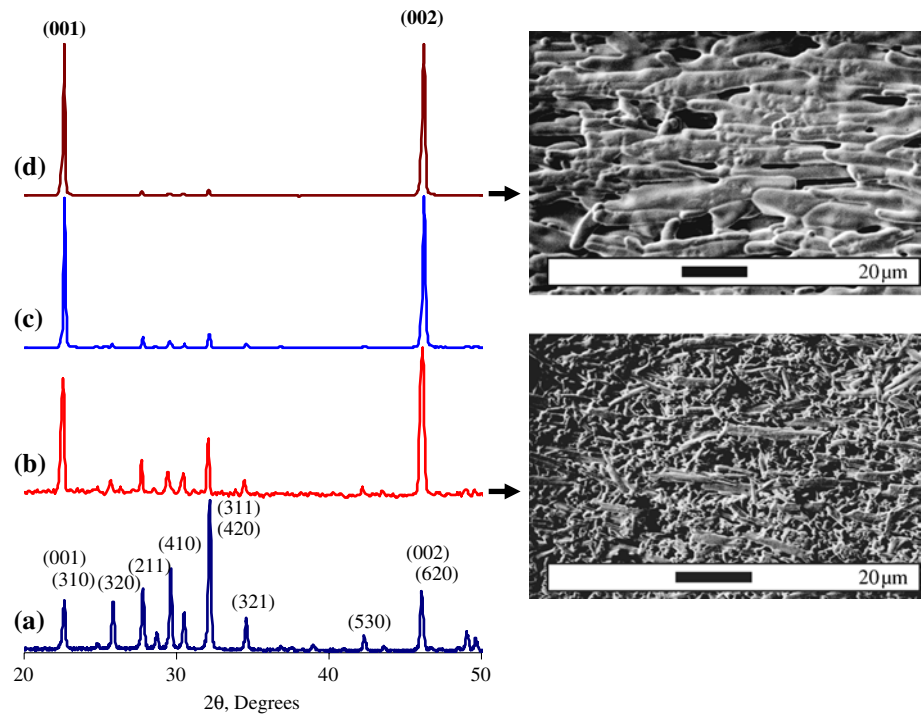


**Fig. 4** Crystallographic (XRD patterns,  $\perp$ -cuts) and morphological (SEM pictures,  $\parallel$ -cuts) texture evolution in the samples sintered at 1450 °C for 2 h; (a) N0-T5, (b) N0-T10 and (c) N0-T15

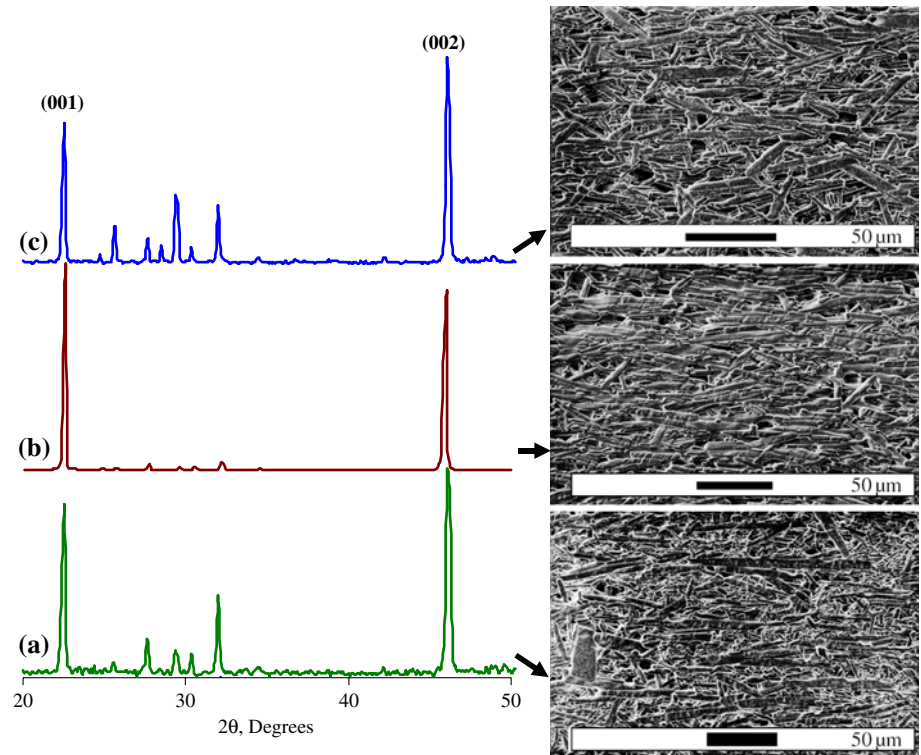
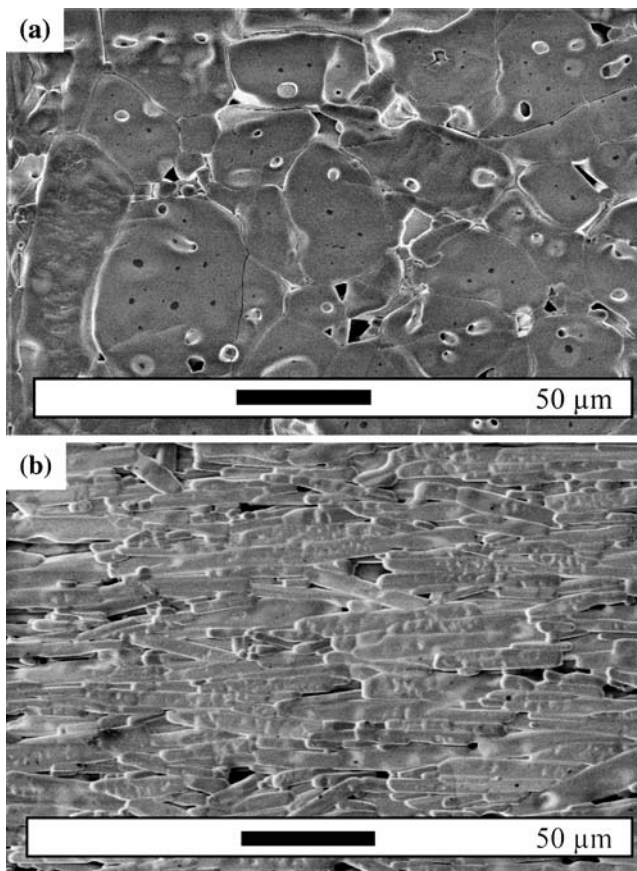


Figure 6 shows the variation of texture fraction,  $f$ , as function of excess  $\text{Nb}_2\text{O}_5$  content (N0-T10, N1-T10, and N1.5-T10) and sintering conditions. As sintering temperature or time increases,  $f$  improves sharply. For example, it is 0.45 at 1350 °C/2 h as compared to 0.96 at 1450 °C/6 h for the N0-T10 samples. In addition,  $f$  in-

creases with the  $\text{Nb}_2\text{O}_5$  content and the increase in  $f$  is more pronounced at lower sintering conditions. For example, it is 0.45 for the N0-T10, 0.56 for the N1-T10 and 0.65 for the N1.5-T10 after sintering at 1350 °C for 2 h. Higher  $f$  can be attributed to the formation of a liquid due to the presence of excess  $\text{Nb}_2\text{O}_5$ , favoring



**Fig. 5** SEM pictures of (a) N1.5-T0 sample sintered at 1400 °C for 2 h and (b) N1.5-T10 sample sintered at 1450 °C for 2 h

faster anisotropic grain growth of the template particles in [001]. The liquid phase in the system promotes faster growth of high-surface-energy planes (e.g., {001} in KSN

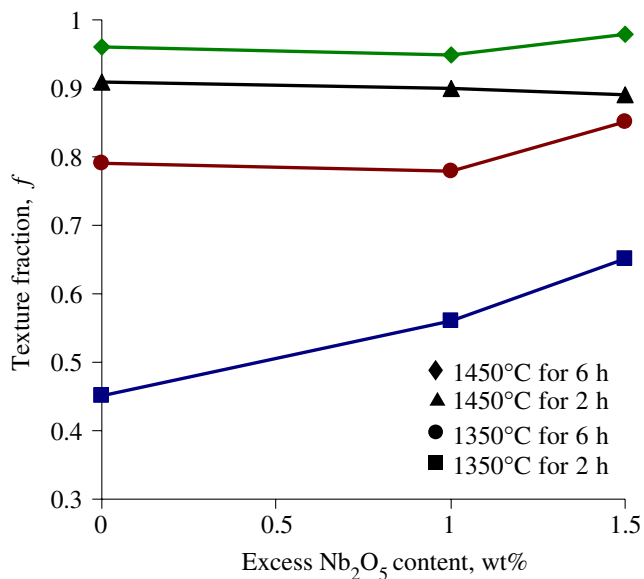


**Fig. 6** Texture fraction as function of excess Nb<sub>2</sub>O<sub>5</sub> content (N0-T10, N1-T10, and N1.5-T10) and sintering conditions

[12, 26]). Growth of the anisotropic grains occurs via solution–reprecipitation, in which small matrix particles dissolve in the liquid phase and then reprecipitate on the larger template particles [8]. Consequently, for a successful TGG, the aspect ratio of the template particles must be high and the matrix grain size must be as fine as possible at the time of densification. An  $f \geq 0.9$  can be obtained at 1450 °C for all samples, even for N0-T10. Local inhomogeneity in chemical composition [1, 4] together with the size effect of the templates over the matrix grains can aid texture development in the N0-T10 samples because  $f$  almost levels off at  $T = 1450$  °C for each set. Microstructures of the N0-T10 and N1.5-T10 samples sintered at 1450 °C for 2 h are shown in Figs. 4b and 5b, respectively. Both graphs reveal highly textured microstructures. In addition, Fig. 4 compares the effect of template concentration on texture development in the samples sintered at 1450 °C for 2 h.  $f$  was calculated to be around 0.6 for the N0-T5 and N0-T15 as compared to 0.91 for the N0-T10. These results indicate that the optimum template content is around 10 wt%.

Texture characterization calculated by the Lotgering factor is an easy method, but it does not provide information about orientation distribution around [001]. Therefore, the distribution was calculated from the rocking curves, using Eq. 2. These curves enable us to calculate degree of orientation parameter,  $r$ , which is closely related to the width of the distribution of textured grains and ranges from  $r = 1$  for random to  $r = 0$  for perfectly textured materials. The  $r$  parameter was calculated to be 0.21 for the N0-T10, 0.31 for the N0-T5 and 0.34 for the N0-T15 samples. In addition, the elongated grains are oriented within 8.4° (i.e., at full width at half maximum) around [001] in the N0-T10, as compared to 15.6° in the N0-T5 and 17.6° in the N0-T15. These results again indicate that 10 wt% template results in a high quality of texture with a narrow distribution of elongated grains in [001] in the reactive TGG of KSN ceramics.

### Ferroelectric properties

Figure 7 compares the polarization–electric field (P–E) hysteresis loops between random and textured samples. The compositions are random N1.5-T0 sample sintered at 1350 °C for 2 h (see Fig. 2c for the SEM picture) and textured N1.5-T10 sample sintered at 1450 °C for 2 h (see Fig. 5b for the SEM picture). The random sample sintered at lower temperature was used in order to eliminate the adverse effect of abnormal grain growth or coarsening on microstructure (similar to the one shown in Fig. 5a). The textured N1.5-T10

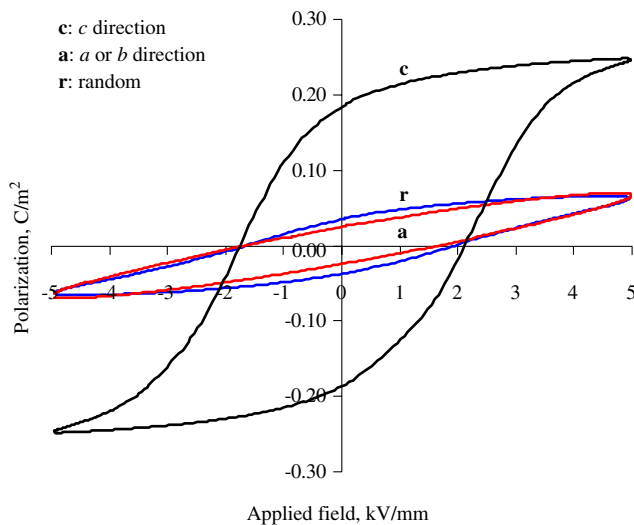


**Fig. 7** P–E loops of random (N1.5-T0) sample sintered 1350 °C for 2 h and textured (N1.5-T10) sample sintered at 1450 °C for 2 h. The **a** and **c** loops are from the textured sample and the **r** loop is from the random sample

sample has an  $f = 0.9$  and a density of 95% TD. The textured sample has a well-saturated P–E loop and show distinct P–E anisotropy between the polar  $c$  direction ([001]) and non-polar  $a$  or  $b$  direction in that remanent polarization ( $P_r$ ) is considerably higher in the former. The  $P_r$  is 0.19 C/m<sup>2</sup> in the polar direction (Curve **c**) as compared to 0.03 C/m<sup>2</sup> in the non-polar direction (Curve **a**) and 0.04 C/m<sup>2</sup> as for the random sample (Curve **r**). The coercive field ( $E_c$ ) is about 2 kV/mm for both samples. The estimated saturation polarization ( $P_{sat}$ ) observed at 5 kV/mm is 0.25 C/m<sup>2</sup> (Curve **c**) which is comparable to reported KSN single crystal value of 0.25 C/m<sup>2</sup> [27]. A very similar P–E hysteresis loop was also recorded from the textured N1.5-T10 sample sintered at 1450 °C for 6 h ( $f = 0.98$ ), stating that an  $f \geq 0.9$  is required to obtain enhanced P–E properties. To our knowledge, this is the first report of enhanced and highly anisotropic electrical properties measured in the KSN ceramics.

In addition, it was observed during the sequential measurement of P–E loops as a function of increasing applied field that polarization increased continuously, stating that there happens no fast polarization fatigue in the samples. Detailed dielectric and piezoelectric properties as a function of texture, additive content and sintering conditions will be reported later.

## Conclusions

<001>-textured KSr<sub>2</sub>Nb<sub>5</sub>O<sub>15</sub> (KSN) ceramics were fabricated successfully in a matrix of SrNb<sub>2</sub>O<sub>6</sub> and

KNbO<sub>3</sub> powders via reactive templated grain growth (TGG), using acicular KSN particles as the template for grain growth in [001]. Excess Nb<sub>2</sub>O<sub>5</sub> was added as a liquid former. The template particles, synthesized by reacting SrNb<sub>2</sub>O<sub>6</sub> with KCl, were used to texture KSN in [001]. Quenching experiments on the template-free samples indicated that KSN phase formation started at 1100 °C and was complete at 1300 °C, regardless of the presence of excess Nb<sub>2</sub>O<sub>5</sub>. However, excess Nb<sub>2</sub>O<sub>5</sub> affected the microstructure evolution in that anisotropic grain growth became more dominant with increasing Nb<sub>2</sub>O<sub>5</sub> content.

Template particles grew at the expense of matrix grains with increasing sintering time and temperature, resulting in improved texture fraction,  $f$ . Samples containing 10 wt% templates reached  $f \geq 0.9$  after sintering 1450 °C for 2 h. A maximum  $f$  obtained in this study was 0.98 in the 1.5 wt% excess Nb<sub>2</sub>O<sub>5</sub>-containing samples (N1.5-T10) sintered at 1450 °C for 6 h. In addition, a template content of 5 wt% was not enough to induce high texture fraction due to the grain growth in the matrix and 15 wt% template content caused tangling of the templates during tape casting. The degree of orientation parameter,  $r$ , was calculated to be 0.21 for the N0-T10, 0.31 for the N0-T5 and 0.34 for the N0-T15 samples. Therefore, 10 wt% template content resulted in a high quality of texture with a narrow distribution of elongated grains in [001]. Template particles controlled matrix grain growth and thus no cracking or abnormal grain growth was observed in the samples textured by reactive TGG.

The remanent polarization,  $P_r$ , was measured to be 0.19 C/m<sup>2</sup> in the polar  $c$  direction ([001]) as compared to 0.03 C/m<sup>2</sup> in the non-polar  $a$  or  $b$  direction and 0.04 C/m<sup>2</sup> as for the random sample. The estimated saturation polarization ( $P_{sat}$ ) was 0.25 C/m<sup>2</sup> which is comparable to reported KSN single crystal value of 0.25 C/m<sup>2</sup>. To our knowledge, this is the first report of enhanced and highly anisotropic electrical properties measured in the KSN ceramics.

**Acknowledgement** The financial support of the Scientific and Technical Research Council of Turkey (TUBITAK, Project #: MISAG 245) is greatly acknowledged.

## References

1. Scott BA, Giess EA, O'kane DF, Burns G (1970) J Am Ceram Soc 53(2):106
2. Neurgaonkar RR, Oliver JR, Cory WK, Cross LE, Viehland D (1994) Ferroelectrics 160:265
3. Bhanumathi A, Murty SN, Umakantham K, Mouli KC, Padmavathi G, Rao KT, Syamalamba V (1990) Ferroelectrics 102:173

4. Kimura T, Miyamoto S, Yamaguchi T (1990) *J Am Cer Soc* 73(1):127
5. Takeuchi T, Tani T, Saito Y (1999) *Jpn J Appl Phys Part I* 38(9B):5553
6. Hong SH, Messing GL (1999) *J Am Ceram Soc* 82(4):867
7. Suvaci E, Messing GL (2000) *J Am Ceram Soc* 83(8):2041
8. Seabaugh MM, Kerscht IH, Messing GL (1997) *J Am Ceram Soc* 80(5):1181
9. Horn JA, Zhang SC, Selvaraj U, Messing GL, Trolier-Mckinstry S (1999) *J Am Ceram Soc* 82(4):921
10. Brahmaroutu B, Messing GL, Trolier-McKinstry S, Selvaraj U (1996) In Kulwicki B, Amin A, Safari A (eds) *Proceedings of the Tenth IEEE Int. Symp. On Appl. of Ferroelectrics*, NJ, 1996, vol 2, p. 883
11. Messing GL, Sabolsky EM, Trolier-McKinstry S, Duran C, Kwon S, Brahmaroutu B, Park P, Yilmaz H, Rehrig PW, Eitel KB, Suvaci E, Seabaugh M (2004) *Crit Rev Solid State Mater Sci* 29:49
12. Kimura T, Saiubol S, Nagata K (1995) *J Ceram Soc Japan Int Ed* 103(2):132
13. Yurdal K, Duran C, Alkoy S, Bakan HI (2004) *Key Eng Mater* 264–268:1285
14. Nagata K, Yamamoto Y, Igarashi H, Okazaki K (1981) *Ferroelectrics* 38:853
15. Neurgaonkar RR, Oliver JR, Nelson JG, Cross LE (1991) *Mat Res Bull* 26:771
16. Huang QW, Zhu LH, Xu J, Wang PL, Gu H, Cheng YB (2005) *J Euro Ceram Soc* 25:957
17. Lee W-J, Fang T-T (1998) *J Am Ceram Soc* 81(4):1019
18. Lee H-Y, Freer R (1997) *J Appl Phys* 81:376
19. Lee H-Y, Freer R (1998) *J Mater Sci* 33:1703
20. Rahaman MN, de Jonghe LC (1993) *J Am Ceram Soc* 76:1739
21. Lotgering FK (1959) *J Inorg Nucl Chem* 9:113
22. Seabaugh MM, Vaudin MD, Cline JP, Messing GL (2000) *J Am Ceram Soc* 83:2049
23. Vaudin MD (1999) *TexturePlus National Institute of Standards and Technology. Ceramics Division, Gaithersburg, MD*
24. March A (1932) *Z Kristallogr* 81:285
25. Dollase WA (1986) *J Appl Crystallogr* 19:267
26. Neurgaonkar RR, Ho WW, Cory WK, Hall WF, Cross LE (1984) *Ferroelectrics* 51:185
27. Neurgaonkar RR, Cory WK, Oliver JR, Sharp EJ, Wood GL, Salamo GJ (1993) *Ferroelectrics* 142:167